

# Inertial- and Dissipation-Range Asymptotics in Fluid Turbulence

Sujan K. Dhar, Anirban Sain, and Rahul Pandit\*

Department of Physics, Indian Institute of Science, Bangalore 560 012, India

We propose and verify a wave-vector-space version of generalized extended self-similarity [R. Benzi *et al.*, *Europhys. Lett.* **32**, 709 (1995)] and broaden its applicability to uncover intriguing, universal scaling in the far dissipation range by computing high-order ( $\leq 20$ ) structure functions numerically for (1) the three-dimensional, incompressible Navier-Stokes equation (with and without hyperviscosity) and (2) the Gledzer-Ohkitani-Yamada shell model for turbulence. Also, in case (2), with Taylor-microscale Reynolds numbers  $4 \times 10^4 \leq \text{Re}_\lambda \leq 3 \times 10^6$ , we find that the inertial-range exponents ( $\zeta_p$ ) of the order- $p$  structure functions do not approach their Kolmogorov value  $p/3$  as  $\text{Re}_\lambda$  increases. [S0031-9007(97)02862-7]

Kolmogorov's pioneering work (K41) [1] on homogeneous isotropic turbulence used the cascade picture to predict simple scaling forms for velocity structure functions (see below). These forms hold for distances  $r$  in the *inertial range* that lies between  $L$ , the forcing scale, and  $\eta_d$ , the dissipation scale at which viscosity starts modifying the invariant energy cascade. Subsequent studies [2–11] have refined K41, as we outline below, but have concentrated principally on the inertial range. In this Letter we use recently developed generalizations of such scaling [2,5] to elucidate the crossover from inertial- to dissipation-range behaviors in fluid turbulence.

The order- $p$  velocity structure functions  $S_p(r) \equiv \langle |\mathbf{v}_i(\mathbf{x} + \mathbf{r}) - \mathbf{v}_i(\mathbf{x})|^p \rangle$ , where  $i$  ( $= 1, 2$ , or  $3$ ) denotes components, scale as  $S_p(r) \sim r^{\zeta_p}$  at high Reynolds numbers  $\text{Re}_\lambda$  and for the inertial range  $20\eta_d \lesssim r \ll L$  (where  $\lambda$  is the Taylor microscale). The K41 result  $\zeta_p = p/3$  works well for  $p \lesssim 4$ ; but for large  $p$ , most studies [2–11] find multiscaling, i.e.,  $\zeta_p = p/3 - \delta\zeta_p$ , a nonlinear increasing function with  $\delta\zeta_p > 0$ . Also, a procedure called extended self-similarity (ESS) [5], in which  $\zeta_p$  is obtained from  $S_p \sim S_3^{\zeta_p}$ , extends the apparent inertial range down to  $r \approx 5\eta_d$ . A more recent technique, generalized extended self-similarity (GESS) [2], uses the dimensionless structure functions  $\mathcal{G}_p(r) \equiv S_p(r)/[S_3(r)]^{p/3}$  and suggests that the form  $\mathcal{G}_p \sim [\mathcal{G}_q]^{\rho_{p,q}}$ , with  $\rho_{p,q} = [\zeta_p - p\zeta_3/3]/[\zeta_q - q\zeta_3/3]$ , holds down to the lowest resolvable values of  $r$ . GESS has been tested [2] to some extent ( $p, q \leq 6$ ). We show that ESS and GESS provide us with sensitive ways of studying the crossover of structure functions from their inertial- to dissipation-range forms.

Specifically, we show how GESS is modified at sufficiently small  $r$  by computing wave-vector-space ( $k$ -space) analogs of high-order ( $\leq 20$ ) structure functions for (1) the three-dimensional, incompressible Navier Stokes equation (3D NS), with and without hyperviscosity, and (2) the Gledzer-Ohkitani-Yamada (GOY) shell model for turbulence [9–12] (where we attain both large  $\text{Re}_\lambda$  and  $k \gg k_d \equiv \eta_d^{-1}$ ). We further propose a  $k$ -space GESS

[2], show that it holds for  $L^{-1} \ll k \lesssim 1.5k_d$ , but then *crosses over to another form in the far dissipation range*. To study this we postulate  $k$ -space ESS [for real-space structure functions we use the symbols  $S$  and  $\mathcal{G}$  and for their  $k$ -space analogs (*not* Fourier transforms) the symbols  $S$  and  $G$ ]:

$$S_p \equiv \langle |\mathbf{v}(\mathbf{k})|^p \rangle \approx A_{I_p}(S_3)^{\zeta'_p}, \quad L^{-1} \ll k \lesssim 1.5k_d,$$

$$S_p \equiv \langle |\mathbf{v}(\mathbf{k})|^p \rangle \approx A_{D_p}(S_3)^{\alpha_p}, \quad 1.5k_d \lesssim k \ll \Lambda, \quad (1)$$

where  $A_{I_p}$  and  $A_{D_p}$  are, respectively, nonuniversal amplitudes for inertial and dissipation ranges and  $\Lambda^{-1}$  the (molecular) length at which hydrodynamics fails (see [5,6] for real-space analogs). Our study shows (Figs. 1 and 2)

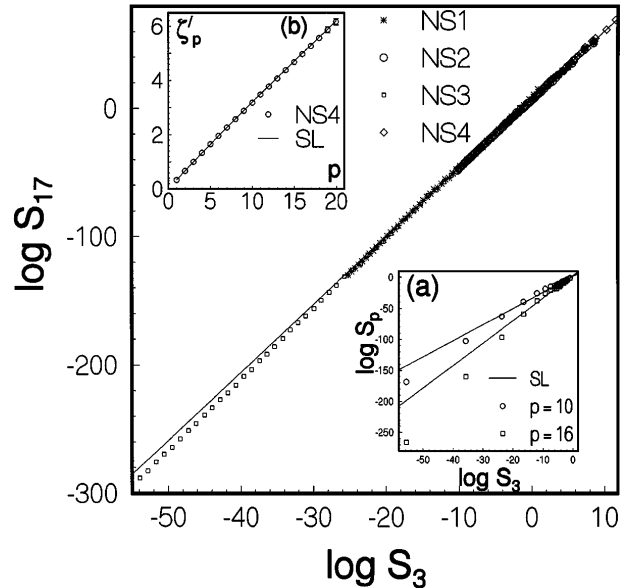


FIG. 1. Log-log plots (base 10) of  $S_p$  versus  $S_3$  for 3D NS ( $p = 17$  for runs NS1-4) and GOY [run G1 in inset (a)] models showing our  $k$ -space ESS [Eq. (1)]; full lines are the SL prediction [4]. Inset (b):  $\zeta'_p$  (circles) from run NS4; the line is  $\zeta'_p = 2(\zeta_p + 3p/2)/11$ , with the  $\zeta_p = \zeta_p^{\text{SL}}$ . Note the deviation of our data points from SL lines at small  $S_3$ , i.e., in the dissipation range; this shows clearly only for NS3 on this scale, but is also present in runs NS1 and NS2 (Fig. 3).

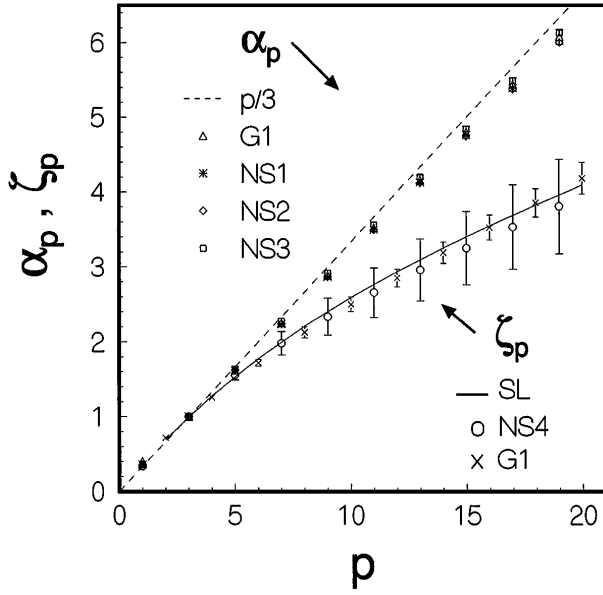


FIG. 2. Inertial- and dissipation-range exponents  $\zeta_p$  and  $\alpha_p$  (extracted from plots like Fig. 1) versus  $p$  for GOY and NS runs and their comparison with the SL formula [4] and  $p/3$ . We obtain  $\zeta_p$  from our measured  $\zeta_p'$  and the formula  $\zeta_p = 11\zeta_p'/2 - 3p/2$ ; this amplifies the error bars relative to Fig. 1(b). Error bars for  $\alpha_p$  are shown but not apparent since they are comparable to the symbol sizes.

that Eq. (1) holds with two different exponents  $\alpha_p$  and  $\zeta_p'$ . In the GOY model  $\zeta_p' = \zeta_p$ , but we find explicitly [Fig. 1(b)] that, for the 3D NS case,  $\zeta_p' = 2(\zeta_p + 3p/2)/11$  [i.e.,  $S_p(k) \sim k^{-(\zeta_p + 3p/2)}$  in the inertial range [13]]; the difference between the two arises because of phase-space factors. Both  $\zeta_p$  and  $\alpha_p$  (Fig. 2) seem universal [the same for all GOY and 3D NS runs (Table I) [14]].  $\zeta_p$  agrees fairly with the She-Leveque (SL) [4] formula  $\zeta_p^{\text{SL}} = p/9 + 2[1 - (2/3)^{p/3}]$  for the ranges of  $p$  and  $\text{Re}_\lambda$  in Fig. 2; and  $\alpha_p$  is close to, but *systematically less* than,  $p/3$ . The  $k$  dependences of the inertial- and dissipation-range asymptotic behaviors follow now from the dependence of  $S_3$  on  $k$ : We find

$$S_3 \approx B_I k^{-\xi_3 - 9/2}, \quad L^{-1} \ll k \lesssim 1.5k_d, \quad (2)$$

$$S_3 \approx B_D k^\delta \exp(-ck/k_d), \quad 1.5k_d \lesssim k \ll \Lambda, \quad (3)$$

where  $B_I$  and  $B_D$  are, respectively, nonuniversal amplitudes [Eq. (2) holds [13] for 3D NS; for GOY the factor 9/2 is absent]. Thus, in the far dissipation range, *all*  $S_p \sim k^{\theta_p} \exp(-c\alpha_p k/k_d)$  for  $1.5k_d \lesssim k \ll \Lambda$ , with  $\theta_p = \alpha_p \delta$ , a form not easy to verify numerically for large  $p$ , given the rapid decay at large  $k$ , and suggested hitherto [15] only for  $S_2$ . In Eq. (3),  $\delta, c, k_d$  are not universal, but we extract the universal part of the crossover via our  $k$ -space GESS: Define  $G_p \equiv S_p/(S_3)^{p/3}$ ; log-log plots of  $G_p$  versus  $G_q$  yield curves [Figs. 3(a) and 3(b)] with asymptotes which have *universal, but different*, slopes in inertial and dissipation ranges. The inertial-range asymptote has a slope  $\rho(p, q)$  (as in real-space

GESS [2] which follows from the formulas above); the resulting  $\zeta_p$  are in fair agreement with the SL formula [4]. The dissipation-range asymptote has a slope  $\omega(p, q) \equiv [\alpha_p - p/3]/[\alpha_q - q/3]$ . The slopes of these asymptotes are universal, but the point at which the curve veers off from the inertial-range asymptote depends on the model (GOY, NS, etc.). However, a simple transformation yields a *universal crossover scaling function* [different for each  $(p, q)$  pair because of multiscaling]: Define  $\log_{10}(H_{pq}) \equiv D_{pq} \log_{10}(G_p)$  and  $\log_{10}(H_{qp}) \equiv D_{qp} \log_{10}(G_q)$ ; the scale factors  $D_{pq} = D_{qp}$  are *nonuniversal*, but plots of  $\log_{10}(H_{pq})$  versus  $\log_{10}(H_{qp})$  show data from *all* GOY and 3D NS runs collapsing onto *one universal curve* within our error bars [Fig. 3(c) for  $p = 6$  and  $q = 9$ ] for *all*  $k$  and  $\text{Re}_\lambda$ . (This transformation holds the G1-8 GESS plots fixed and stretches the NS plots, without changing their slopes, until the asymptotes match.) Both ESS (Fig. 1) and GESS (Fig. 3) remove the exponential *controlling factor* [16] from the *leading asymptotic behavior* of  $S_p$  in the far dissipation range and expose the remaining power-law dependence on  $k$ . Also, it is easy to see analytically that GESS plots (Fig. 3) amplify slope differences between inertial- and dissipation-range asymptotes relative to ESS plots (Fig. 1).

How robust is the fair agreement of  $\zeta_p$  (Fig. 2) with the SL formula? Some studies [17–19] suggest that, as  $\text{Re}_\lambda \rightarrow \infty$ ,  $\delta\zeta_p \equiv (p/3 - \zeta_p) \rightarrow 0$ . Numerical solutions of the 3D NS equation can at best achieve [7–20]  $\text{Re}_\lambda \lesssim 220$ , too small, by far, to resolve this issue, so we address it for the GOY model by studying the range  $4 \times 10^4 \lesssim \text{Re}_\lambda \lesssim 3 \times 10^6$ . We find (Fig. 4) that  $\delta\zeta_p$  does not vanish with increasing  $\text{Re}_\lambda$ , but rises marginally [21]. Systematic experiments at high  $\text{Re}_\lambda$  can check if the trends of Fig. 4 obtain in the NS case.

We remark that if we *assume* the hierarchy  $[G_{p+1}/G_p] = [G_p/G_{p-1}]^\gamma [\lim_{p \rightarrow \infty} G_{p+1}/G_p]^{1-\gamma}$  with  $\gamma^3 = 2/3$  (whose real-space analog is equivalent [2] to the SL moment hierarchy for the energy dissipation [4]) and use [22]  $G_p(k) \approx C_p k^{\beta_p}$ , we get a difference equation for  $\beta_p$  *identical* to the SL one (our  $\beta_p$  is their  $-\tau_{p/3}$ ). This, when solved with the boundary conditions  $\beta_0 = \beta_3 = 0$  and  $\lim_{p \rightarrow \infty} (\beta_{p+1} - \beta_p) = 2/9$ , yields the SL formula (via  $\zeta_p = -\beta_p + p\zeta_3/3$ ). However, our GESS yields  $[G_{p+1}/G_p] \approx C_p' [G_p/G_{p-1}]^{Y_p}$  with  $Y_p = (\zeta_{p+1} - \zeta_p - 1/3)/(\zeta_p - \zeta_{p-1} - 1/3)$ . Superficially, this might seem to violate the hierarchy assumed above, but it turns out to be consistent with our GESS form, if  $Y_p = \gamma - 2(1 - \gamma)/[9(\zeta_p - \zeta_{p-1} - \zeta_3/3)]$ , which is precisely the SL difference equation. Of course, our GESS form can hold with  $\zeta_p \neq \zeta_p^{\text{SL}}$ ; Fig. 2 shows the quality of agreement between our measured  $\zeta_p$  and  $\zeta_p^{\text{SL}}$ .

We use a pseudospectral method [7] to solve the incompressible 3D NS equation. We force the first two  $k$  shells, use a box with side  $L_B = \pi$  and  $64^3$  modes. Our dissipation term  $-(\nu + \nu_H k^2)k^2$  allows for both viscosity  $\nu$  and hyperviscosity  $\nu_H$ . For time integration

TABLE I. Parameters  $\nu$  (viscosity),  $\nu_H$  (hyperviscosity),  $\text{Re}_\lambda$  (Taylor-microscale Reynolds number),  $\tau_e$  (box-size eddy-turnover time),  $\tau_{\text{av}}$  (averaging time),  $\tau_t$  (transient time), and  $k_d$  (dissipation-scale wave number) for our 3D NS runs NS1-4 ( $k_{\text{max}} = 64$ ) and GOY-model runs G1-8 ( $k_{\text{max}} = 2^{22}k_0$ ). The step size ( $\delta t$ ) used is 0.02 for NS1-4,  $10^{-4}$  for G1-4, and  $2 \times 10^{-5}$  for G5-8. Note  $\tau_e \approx 8\tau_t$ , the integral time for our NS runs.

Run	$\nu$	$\nu_H$	$\text{Re}_\lambda$	$\tau_e/\delta t$	$\tau_t/\tau_e$	$\tau_{\text{av}}/\tau_e$	$k_{\text{max}}/k_d$
NS1	$5 \times 10^{-4}$	0	$\approx 3.5$	$\approx 3 \times 10^4$	$\approx 1$	2	$\approx 4$
NS2	$2 \times 10^{-4}$	0	$\approx 8$	$\approx 3 \times 10^4$	$\approx 1$	$\approx 2.5$	$\approx 2.3$
NS3	$5 \times 10^{-4}$	$5 \times 10^{-6}$	$\approx 3.5$	$\approx 3 \times 10^4$	$\approx 1$	$\approx 1$	$\approx 6.5$
NS4	$5 \times 10^{-4}$	$10^{-6}$	$\approx 22$	$\approx 3 \times 10^3$	$\approx 10$	$\approx 7$	$\approx 2$
G1-4	$5 \times 10^{-6} - 10^{-7}$	0	$4 \times 10^4 - 3 \times 10^5$	$\approx (1.5 - 2.0) \times 10^4$	$\approx 500$	$\approx 2500$	$\approx 2^5 - 2^3$
G5-8	$5 \times 10^{-8} - 10^{-9}$	0	$3.5 \times 10^5 - 3 \times 10^6$	$\approx (0.7 - 1) \times 10^5$	$\approx 500$	$\approx 2500$	$\approx 2^3 - 1$

we use an Adams-Bashforth scheme (step size  $\delta t$ ) [7]. Parameters for our 3D NS runs NS1-4 are given in Table I, where  $\tau_e \equiv L_B/v_{\text{rms}}$  is the box-size eddy-turnover time and  $\tau_{\text{av}}$  the averaging time, after initial transients have decayed over a period  $\tau_t$ . We use  $\text{Re}_\lambda = v_{\text{rms}}\lambda/\nu$ , where  $\lambda = [\int_0^\infty E(k) dk / \int_0^\infty k^2 E(k) dk]^{1/2}$ ,  $v_{\text{rms}} = [(2/3L_B^3) \int_0^\infty E(k) dk]^{1/2}$ , and  $E(k) \sim S_2(k)k^2$ . All  $S_p(k)$  are averaged over shells of radius  $k$ . Care must be exercised in choosing  $\delta t$  and the forcing amplitude, otherwise there is a slow but systematic stretching of the points along the asymptotes in Figs. 1 and 3 with increasing  $\tau_{\text{av}}$  (over the time scales of our low- $\text{Re}_\lambda$  NS runs). Fortunately, this hardly affects our exponents: Any attendant systematic errors in Fig. 2 are certainly less than the random errors indicated. All our NS runs use quadruple-precision arithmetic and we have checked that halving our integration time step does not affect our results perceptibly. Note also that sample fluctuations over even a few orders of magnitude are unimportant, given the range of our log-log plots like Fig. 1. Also, the agreement between our GOY and NS runs confirms our results. Our GOY-model data are, of course, of much better quality. Here Fourier components of the velocity are labeled by a discrete set of wave vectors  $k_n = k_0 q^n$ . The dynamical variables are the *complex, scalar* velocities  $v_n$  for each shell  $n$ ;  $v_n$  is affected directly only by the velocities in nearest and next-nearest shells. This model yields scaling properties [9–12] akin to experimental ones. The GOY-model equations are

$$\frac{d}{dt} v_n = iC_n - \nu k_n^2 v_n + f_n, \quad (4)$$

where  $\nu$  is the kinematic viscosity,  $f_n$  the external force on shell  $n$ ,  $C_n = (ak_n v_{n+1} v_{n+2} + bk_{n-1} v_{n-1} v_{n+1} + ck_{n-2} v_{n-1} v_{n-2})^*$ , and  $a$ ,  $b$ , and  $c$  can be fixed up to a constant by demanding [11], for  $\nu$ ,  $f_n = 0$ , that  $v_n \sim k_n^{-1/3}$  be a stationary solution of Eq. (4), and the GOY-model kinetic energy and helicity be conserved. We adopt the conventional parameters [10,11]  $k_0 = 2^{-4}$ ,  $q = 2$ ,  $a = 1$ ,  $b = c = -1/2$ , and use  $f_n = 5 \times 10^{-3}(1+i)\delta_{n,1}$ , i.e., we force the first shell [23]. The GOY-model structure functions are  $S_{n,p} \equiv \langle |v_n|^p \rangle \sim k_n^{-\zeta_p}$  [9–11]; reliable values of  $\zeta_p$  obtain [11] if we use  $\Sigma_{n,p} = \langle |\text{Im}[v_n v_{n+1} v_{n+2} + v_{n-1} v_n v_{n+1}/4]|^p \rangle^{1/3}$  since this removes an underlying three cycle. We have used  $\Sigma_{n,p}$  to obtain Fig. 4 [24], but  $S_{n,p}$  in Figs. 1–3 for consistency with 3D NS. We use an Adams-Bashforth scheme [10] (step size  $\delta t$ ) to integrate Eq. (4). The average of the time scale associated with the smallest wave number  $(|v_1|k_1)^{-1}$  gives the “box-size” eddy turnover time. Table I lists other parameters for our 8 GOY-model runs G1–8, for which we use (cf. [10])  $E(k) = S_{n,2}/k_n$ ,  $\lambda = 2\pi/k_0[\Sigma_n S_{n,2}/\Sigma_n k_n^2 S_{n,2}]^{1/2}$ , and  $v_{\text{rms}} = [k_0 \Sigma_n S_{n,2}/\pi]^{1/2}$ . This yields  $\text{Re}_\lambda \sim \nu^{-0.5}$ , as expected [25] at large  $\text{Re}_\lambda$ . Our GOY model runs are done using double-precision arithmetic, but we have repeated run G1 in quadruple precision and checked that our results are unchanged.

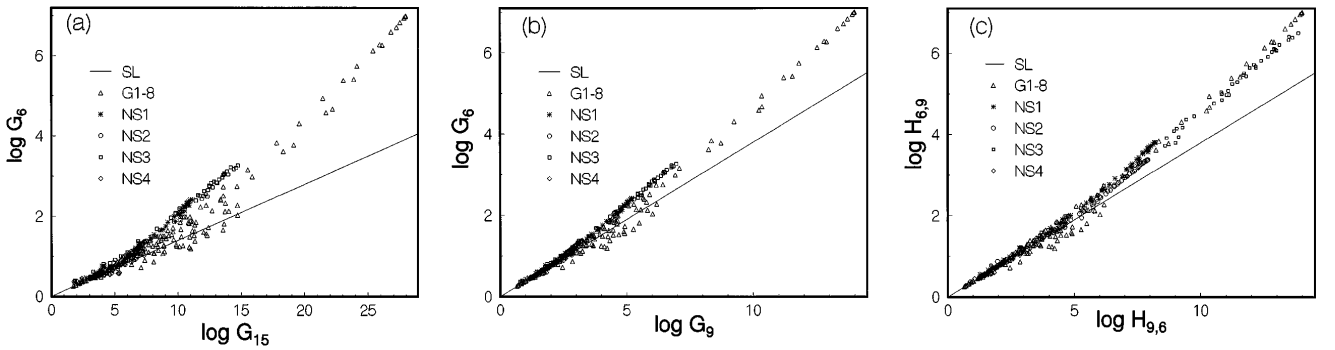


FIG. 3. Log-log (base 10) plots of  $G_6$  versus (a)  $G_{15}$  and (b)  $G_9$  illustrating our  $k$ -space GESS; (c)  $H_{6,9}$  versus  $H_{9,6}$  showing the universal inertial- to dissipation-range crossover (see text). The line shows the SL, inertial-range prediction.

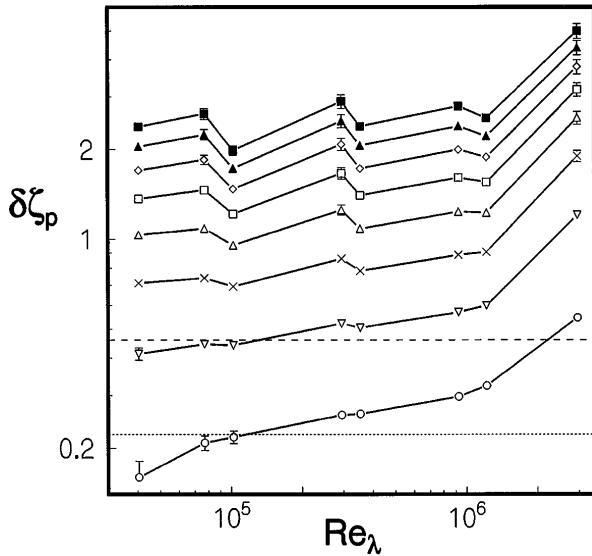


FIG. 4. Log-log plot (base 10) of  $\delta\zeta_p$  versus the Taylor-microscale Reynolds number  $Re_\lambda$  for our GOY runs (G1-8) with  $p = 6, 8, \dots, 20$  (from bottom to top). The dotted ( $p = 6$ ) and dashed ( $p = 8$ ) lines show the SL results [4]. Error bars are shown but are often smaller than the symbol sizes.

Experimental evidence for the slope change in the dissipation range in real-space analogs of Fig. 1 was given by Stolovitzky and Sreenivasan [6], who postulated  $S_p \sim S_3^{\alpha'_p}$  in the dissipation range and suggested  $\alpha'_p \approx (\zeta_{3p/2} + p/2)/(\zeta_{9/2} + 3/2)$ . We have not been able to obtain a simple relation between our  $\alpha_p$  and their  $\alpha'_p$  (unlike [13] that between  $\zeta_p$  and  $\zeta'_p$ ) since  $S_p$  does not have a power-law dependence on  $k$  in the dissipation range.

In conclusion, then, we have used our  $k$ -space ESS and GESS to obtain universal inertial-to-dissipation-range crossover in structure functions. It would be interesting to test this novel *universality* of dissipation-range asymptotics in different flows. The multiscaling we find in the far dissipation range might, at first sight, seem surprising because dissipation dominates here, but, as has been noted earlier [15], the intermittency seen in the far dissipation range can plausibly enhance mean nonlinear transfer even at low  $Re_\lambda$ . Our dissipation-range multiscaling is a manifestation of such intermittency. Preliminary studies [26] yield similar phenomena in MHD turbulence.

We thank S. Ramaswamy for discussions, CSIR and BRNS (India) for support, and SERC (IISc, Bangalore) for computational resources.

\*Also at Jawaharlal Nehru Centre for Advanced Scientific Research, Bangalore, India.

- [1] A. N. Kolmogorov, C. R. Acad. Sci. USSR **30**, 301 (1941).
- [2] R. Benzi, L. Biferale, S. Ciliberto, M. Struglia, and R. Tripiccion, Europhys. Lett. **32**, 709 (1995).
- [3] F. Anselmet, Y. Gagne, E. J. Hopfinger, and R. A. Antonia, J. Fluid Mech. **140**, 63 (1984).

- [4] Z. S. She and E. Leveque, Phys. Rev. Lett. **72**, 336 (1994).
- [5] R. Benzi, S. Ciliberto, R. Tripiccion, C. Baudet, F. Massaioli, and S. Succi, Phys. Rev. E **48**, R29 (1993).
- [6] G. Stolovitzky and K. R. Sreenivasan, Phys. Rev. E **48**, R33 (1993).
- [7] M. Meneguzzi and A. Vincent, in *Advances in Turbulence 3*, edited by A. V. Johansson and P. H. Alfredsson (Springer, Berlin, 1991), pp. 211–220.
- [8] J. Herweijer and W. van de Water, Phys. Rev. Lett. **74**, 4651 (1995).
- [9] M. H. Jensen, G. Paladin, and A. Vulpiani, Phys. Rev. A **43**, 798 (1991).
- [10] D. Pisarenko, L. Biferale, D. Courvoisier, U. Frisch, and M. Vergassola, Phys. Fluids A **5**, 2533 (1993).
- [11] L. Kadanoff, D. Lohse, J. Wang, and R. Benzi, Phys. Fluids **7**, 617 (1995).
- [12] E. B. Gledzer, Sov. Phys. Dokl. **18**, 216 (1973); K. Ohkitani and M. Yamada, Prog. Theor. Phys. **81**, 329 (1989).
- [13] This result is new. Our NS runs, though restricted to relatively low  $Re_\lambda$  ( $\leq 22$ ), uncover it via ESS and  $\zeta_3 = 1$ . For  $p$  even this result follows via dimensional analysis if one Fourier transforms the real-space  $S_p$  and makes the numerically plausible *assumption* that  $\langle \mathbf{v}_{i1}(\mathbf{k}_1), \dots, \mathbf{v}_{ip}(\mathbf{k}_p) \rangle$  is dominated by terms in which the  $\mathbf{k}_m$ ,  $m = 1, \dots, p$  arguments form equal and opposite pairs *all* with magnitude  $k$ , i.e.,  $\langle \mathbf{v}_{i1}(\mathbf{k}_1), \dots, \mathbf{v}_{ip}(\mathbf{k}_p) \rangle \sim S_p(k) [\delta(\mathbf{k}_1 + \mathbf{k}_2) \cdots \delta(\mathbf{k}_{p-1} + \mathbf{k}_p) + \text{permutations}]$ . Other authors [27] make this assumption, but use further approximations to obtain different results.
- [14] With  $-\nu_H k^{\alpha_H}$  dissipation,  $\zeta_p$  depend on  $\alpha_H$ ; this nonuniversality is removed in plots like Fig. 3, at least in the inertial range [E. Leveque and Z. S. She, Phys. Rev. Lett. **75**, 2690 (1995); V. Borue and S. A. Orszag, Europhys. Lett. **29**, 6875 (1995)]. With our  $-(\nu k^2 + \nu_H k^{\alpha_H})$  dissipation,  $\nu \neq 0$  and  $2 < \alpha_H$ , so  $\nu$ , not  $\nu_H$ , controls  $\zeta_p$ .
- [15] S. Chen, G. Doolen, J. R. Herring, R. H. Kraichnan, S. A. Orszag, and Z. S. She, Phys. Rev. Lett. **70**, 3051 (1993).
- [16] C. M. Bender and S. A. Orszag, *Advanced Mathematical Methods for Scientists and Engineers* (McGraw-Hill, New York, 1978), p. 80.
- [17] T. Katsuyama, Y. Horiuchi, and K. Nagata, Phys. Rev. E **49**, 4052 (1994).
- [18] S. Grossman, D. Lohse, V. L'vov, and I. Procaccia, Phys. Rev. Lett. **73**, 432 (1994).
- [19] V. S. L'vov and I. Procaccia, Phys. Rev. Lett. **74**, 2690 (1995).
- [20] S. Chen, G. D. Doolen, R. H. Kraichnan, and L. -P. Wang, Phys. Rev. Lett. **74**, 1755 (1995).
- [21] The increase in  $\delta\zeta_p$  for run G8 did not go away on reducing  $\delta t$  to  $4 \times 10^{-6}$ , with  $\tau_t \approx 500\tau_e$  and  $\tau_{av} \approx 2500\tau_e$ .
- [22] In the dissipation range,  $G_p \sim k^{\beta'_p} \exp(-c'_p k/k_d)$ , so there is no SL analog for  $\alpha_p$ .
- [23] This increases the inertial range by 2–3 octaves relative to forcing the fourth shell [10,11].
- [24]  $\Sigma_{n,p}$  yields a slightly lower estimate for  $\zeta_p$  than  $S_{n,p}$ .
- [25] D. Lohse, Phys. Rev. Lett. **73**, 3223 (1994).
- [26] A. Basu, S. K. Dhar, A. Sain, and R. Pandit (unpublished).
- [27] V. S. L'vov, Phys. Rep. **207**, 1 (1991); V. S. L'vov and I. Procaccia, Phys. Rev. E **49**, 4044 (1994).